

Theory of magic optical traps for Zeeman-insensitive clock transitions in alkali-metal atoms

Andrei Derevianko*

Department of Physics, University of Nevada, Reno, Nevada 89557, USA

(Received 16 December 2009; published 20 May 2010)

Precision measurements and quantum-information processing with cold atoms may benefit from trapping atoms with specially engineered, “magic” optical fields. At the magic trapping conditions, the relevant atomic properties remain immune to strong perturbations by the trapping fields. Here we develop a theoretical analysis of magic trapping for especially valuable Zeeman-insensitive clock transitions in alkali-metal atoms. The involved mechanism relies on applying a magic bias B field along a circularly polarized trapping laser field. We map out these B fields as a function of trapping laser wavelength for all commonly used alkalis. We also highlight a common error in evaluating Stark shifts of hyperfine manifolds.

DOI: [10.1103/PhysRevA.81.051606](https://doi.org/10.1103/PhysRevA.81.051606)

PACS number(s): 67.85.-d, 37.10.Jk, 06.30.Ft

A recurring theme in modern precision measurements and quantum-information processing with cold atoms and molecules are the so-called magic traps [1]. At the magic trapping conditions, the relevant atomic properties remain immune to strong perturbations by optical trapping fields. For example, in optical lattice clocks, the atoms are held using laser fields operating at magic wavelengths [2]. The clock levels are shifted due to the dynamic Stark effect that depends on the trapping laser wavelength. At the specially chosen, magic wavelength, both clock levels are perturbed identically; therefore the differential effect of trapping fields simply vanishes for the clock transition. This turned out to be a powerful idea: lattice clocks based on the alkaline-earth-metal atom Sr have recently outperformed the primary frequency standards [3].

Finding similar magic conditions for ubiquitous alkali-metal atoms employed in a majority of cold-atom experiments remains an open challenge. Especially valuable are the microwave transitions in the ground-state hyperfine manifold. Finding magic conditions here, for example, would enable developing micromagic clocks [4]: microwave clocks with the active clockwork area of a few micrometers across. In addition, the hyperfine manifolds are used to store quantum information in a large fraction of quantum-computing proposals with ultracold alkalis. Here the strong perturbation due to trapping fields is detrimental. Namely, the dynamic differential Stark shift is the limiting experimental factor for realizing long-lived quantum memory [5]. Qualitatively, as an atom moves in the trap, it randomly samples various intensities of the laser field; this leads to an accumulation of uncontrolled phase difference between the two qubit states. For very cold samples, the accumulation of uncontrolled phases may arise because the interrogation by the microwaves is an ensemble average over the spatial distribution of atoms across the trap. Magic conditions rectify these problems, as both qubit states see the very same optical potential and do not accumulate differential phase at all. In other words, we engineer a decoherence-free trap.

Initial steps in identifying magic conditions for hyperfine transitions in alkali-metal atoms have been made in Refs. [6–8]. The proposals [7,8] identified magic-wavelength conditions for $M_F \neq 0$ states. Due to nonvanishing magnetic moments, these states, however, are sensitive to stray magnetic fields which would lead to clock inaccuracies and decoherences (except for special cases of relatively large bias fields, see below). Recently, it has been realized by Lundblad *et al.* [9] that magic conditions may be attained for the Zeeman-insensitive $M_F = 0$ states as well. Here the bias magnetic field is tuned to make the conditions magic for a given trapping laser wavelength. These authors experimentally demonstrated these conditions for lattice-confined Rb atoms at a single wavelength. As demonstrated below, mapping out values of magic bias B fields for a wide range of wavelengths requires full-scale structure calculations. Below, I carry out such calculations and point out common pitfalls in evaluating differential polarizabilities of hyperfine manifolds.

In this work, we are interested in the clock transition of frequency ν_0 between two hyperfine states $|F' = I + 1/2, M'_F = 0\rangle$ and $|F = I - 1/2, M_F = 0\rangle$ attached to the ground electronic $nS_{1/2}$ state of an alkali-metal atom (I is the nuclear spin). Here and below we denote the upper clock state as $|F'\rangle$ and the lower state as $|F\rangle$. The magic-wavelength conditions are defined as the clock frequency being independent of the perturbing trapping optical field.

We start by reviewing the Zeeman effect for the clock states. The Zeeman Hamiltonian reads $H^Z = -\mu_z B$, μ being the magnetic moment operator. The permanent magnetic moments of the $M_F = 0$ states vanish, so the effect arises in the second order. We need to diagonalize the following Hamiltonian

$$H_{\text{eff}}^Z = \begin{pmatrix} h\nu_0 & H_{F'F}^Z \\ H_{FF'}^Z & 0 \end{pmatrix}. \quad (1)$$

The leading effect is due to off-diagonal coupling $H_{F'F}^Z = \langle F', M'_F = 0 | H^Z | F, M_F = 0 \rangle$. In the case of alkalis, $(\mu_z)_{FF'} \approx \mu_B$, where μ_B is the Bohr magneton. The resulting Zeeman substates repeal each other, and in sufficiently weak B fields,

*andrei@unr.edu

$\mu_B B \ll h\nu_0$, the shift of the transition frequency is quadratic in magnetic field,

$$\frac{\delta\nu_Z(B)}{\nu_0} \approx 2 \left(\frac{\mu_B}{h\nu_0} B \right)^2. \quad (2)$$

Since atoms are trapped by a laser field, the atomic levels are shifted due to the dynamic Stark effect (see, e.g., a review [10]). The relevant energy-shift operator reads

$$\hat{U}(\omega_L) = -\hat{\alpha}(\omega_L) \left(\frac{E_L}{2} \right)^2,$$

where E_L is the amplitude of the laser field and $\hat{\alpha}(\omega_L)$ is the operator of dynamic atomic polarizability; it depends on the laser frequency. Notice that \hat{U} may have both diagonal and off-diagonal matrix elements between atomic states of the same parity.

Now we add the Stark shift couplings to the Hamiltonian (1). The Stark shift operator has both the diagonal and off-diagonal matrix elements in the clock basis. To find the perturbed energy levels, we diagonalize the effective Hamiltonian

$$H_{\text{eff}} = \begin{pmatrix} h\nu_0 + U_{F'F'} & U_{F'F} + H_{F'F}^Z \\ U_{FF'} + H_{FF'}^Z & U_{FF} \end{pmatrix}. \quad (3)$$

For sufficiently weak fields, the resulting shift of the clock frequency reads

$$\delta\nu_{\text{clock}}(\omega_L, B, E_L) = \delta\nu_Z(B) + \delta\nu_S(\omega_L, B, E_L), \quad (4)$$

with the Stark shift

$$\delta\nu_S(\omega_L, B, E_L) = \frac{1}{h} \left\{ \alpha_{F'F'}(\omega_L) - \alpha_{FF}(\omega_L) - \left(\frac{4\mu_{FF'} B}{h\nu_0} \right) \alpha_{F'F}(\omega_L) \right\} \left(\frac{E_L}{2} \right)^2. \quad (5)$$

The magic conditions are attained when $\delta\nu_S(\omega_L, B, E_L) = 0$ for any value of the laser amplitude, i.e., simply when the combination inside the curly brackets vanishes.

At this point one may evaluate the dynamic polarizabilities and deduce the magic B field. Before proceeding with the analysis, I would like to address common pitfalls in evaluating polarizabilities of hyperfine-manifold states, so the reader appreciates the necessity of full-scale calculations. A generic expression for the polarizability of the $|nFM_F\rangle$ state reads

$$\alpha_{FF}^{(0)}(\omega) = \sum_{i=|n_i F_i M_i\rangle} \frac{\langle nFM_F | D_z | i \rangle \langle i | D_z | nFM_F \rangle}{E_{nFM_F} - E_i + \omega} + \dots, \quad (6)$$

where the omitted term differs by $\omega \rightarrow -\omega$, and D is the dipole operator. All the involved states are the hyperfine states. While this requires that the energies include hyperfine splittings, it also means that the wave functions incorporate hyperfine interaction (HFI) to all orders of perturbation theory. Including the experimentally known hyperfine splittings in the summations is straightforward, and unsophisticated practitioners stop at that, completely neglecting the HFI corrections to the wave functions. This is hardly justified, as both contributions are of the same order.

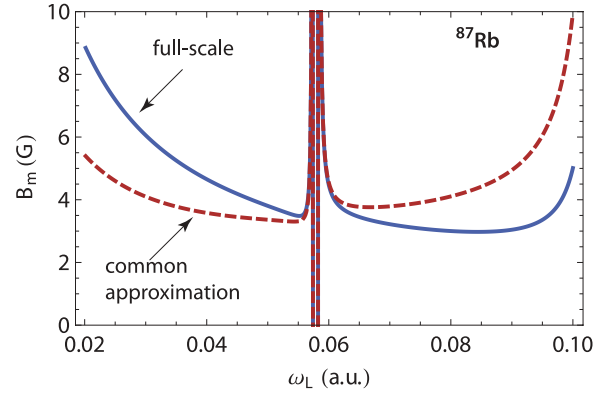


FIG. 1. (Color online) Importance of full-scale calculations. Dependence of magic B field (in G) on laser frequency (in atomic units) for ^{87}Rb . Full-scale calculations (solid blue line) are compared with approximate “experimentalist” computations which neglect the HFI contribution to atomic wave functions (dashed red line).

I would like to remind the reader of a recent controversy: neglecting the HFI correction to wave functions has already led to a (even qualitatively) wrong identification of magic conditions. The authors of Ref. [11] employed the simplified approach and (for $B = 0$) found a multitude of magic wavelengths for clock transitions in Cs. The prediction was in contradiction with a subsequent fountain clock measurement; the full-scale calculations have found that in fact there are no magic wavelengths at $B = 0$, Ref. [6]. To reinforce this point in the context of this paper, in Fig. 1, I compare the results of two calculations of magic B fields for ^{87}Rb as a function of laser frequency. In the first calculation, I neglected the HFI correction to the wave functions (while including the hyperfine corrections to the energies), and the second result comes from the full-scale calculation described below. We clearly see that the simplified approach is off by as much as a factor of 2. Only near the resonance do the two approaches produce similar results.

These two examples should convince the reader that the full-scale calculations are indeed required for reliably predicting magic fields. A consistent approach to evaluating dynamic polarizabilities of hyperfine states was developed in Ref. [6]. The HFI correction to wave functions and energies was included to the leading order; this leads to a third-order analysis quadratic in dipole couplings and linear in the HFI. Below I simplify the magic field conditions using the formalism of Ref. [6].

We may decompose the polarizability into a sum over 0-, 1-, and 2-rank tensors:

$$\hat{\alpha}(\omega_L) = \hat{\alpha}^{(0)}(\omega_L) + A\hat{\alpha}^{(1)}(\omega_L) + \hat{\alpha}^{(2)}(\omega_L). \quad (7)$$

These terms are conventionally referred to as the scalar, vector (axial), and tensor contributions. We also explicitly factored out the degree of circular polarization A of the wave ($A = \pm 1$ for pure σ_{\pm} light). The direction of the bias B field defines the quantization axis. We also fixed the direction of the wave propagation $\hat{\mathbf{k}}$ to be parallel to the B field. Notice that the circular polarization of the optical field is defined with respect to the quantization axis (not $\hat{\mathbf{k}}$).

Below we show that the magic value of the magnetic field may be represented as

$$B_m(\omega_L) \approx -\frac{1}{\mu_B} \frac{2I+1}{2I} \frac{\alpha_{FF}^{(0),\text{HFI}}(\omega_L)}{A\alpha_{nS_{1/2}}^a(\omega_L)} \hbar\nu_0. \quad (8)$$

It depends on the laser frequency and the degree of circular polarization A , $|A| \leq 1$. $\alpha_{FF}^{(0),\text{HFI}}(\omega_L)$ is the scalar HFI-mediated third-order polarizability of the lower clock state, $F = I - 1/2$.

Indeed, the nonvanishing contribution to the differential polarizability $\Delta\alpha(\omega_L) = \alpha_{F'F'}(\omega_L) - \alpha_{FF}(\omega_L)$, entering Eq. (5), comes only through the hyperfine-mediated interactions: $\Delta\alpha(\omega_L) = \alpha_{F'F'}^{\text{HFI}}(\omega_L) - \alpha_{FF}^{\text{HFI}}(\omega_L)$. This reflects the fact that both hyperfine levels belong to the same electronic configuration—the symmetry in responding to fields is only broken when the HFI is included. Moreover, for alkali metals, α_{FF} and $\alpha_{F'F'}$ are dominated by the *scalar* part of polarizability: $\Delta\alpha(\omega_L) \approx \alpha_{F'F'}^{(0),\text{HFI}}(\omega_L) - \alpha_{FF}^{(0),\text{HFI}}(\omega_L)$. These two polarizabilities never intersect; they are strictly proportional to each other: $\alpha_{F'F'}^{(0),\text{HFI}}(\omega_L) = -(I+1)/I \alpha_{FF}^{(0),\text{HFI}}(\omega_L)$.

Now we turn to simplifying the off-diagonal matrix element $\alpha_{F'F}(\omega_L)$ entering Eq. (5). It is dominated by the vector part of polarizability. Indeed, $\langle F', M_F' | \hat{\alpha}^{(0)} | F, M_F \rangle = 0$ due to the angular selection rules ($F' \neq F$). While the tensor contribution $\langle F', M_F' | \hat{\alpha}^{(2)} | F, M_F \rangle$ does not vanish, the electronic momentum of the ground state $nS_{1/2}$ is $J = 1/2$; therefore (since $\langle J = 1/2 | \hat{\alpha}^{(2)} | J = 1/2 \rangle \equiv 0$) this matrix element requires the HFI admixture and becomes strongly suppressed. By contrast, the vector contribution $\langle F', M_F' | \hat{\alpha}^{(1)} | F, M_F \rangle$ does not vanish even if the hyperfine couplings are neglected. It is worth mentioning that it arises only due to relativistic effects, since the orbital angular momentum $L = 0$ for the ground state; e.g., vector polarizability is much smaller in Li than in Cs. The off-diagonal matrix element of the rank-1 polarizability may be expressed as $\alpha_{F'F}^{(1)}(\omega_L) = \frac{1}{2} \alpha_{nS_{1/2}}^a(\omega_L)$, where $\alpha_J^a(\omega_L)$ is the conventionally defined second-order vector polarizability of the ground $nS_{1/2}$ state.

To evaluate the polarizabilities, we used a blend of relativistic many-body techniques of atomic structure, as described in [12]. To improve upon the accuracy, high-precision experimental data were used where available. To ensure the quality of the calculations, a comparison with the experimental literature data on static Stark shifts of the clock transitions was made. Overall, we expect the theoretical errors to not exceed 1% for Cs and to be at the level of a few 0.1% for lighter alkalis. If required, better accuracies may be reached with many-body methods developed for analyzing atomic parity violation [13].

Our computed dependence of the magic B field on laser frequency for representative alkalis (^{23}Na , ^{87}Rb , and ^{133}Cs) is shown in Fig. 2. We also carried out similar calculations for ^{39}K and ^7Li . Results for several laser wavelengths are presented in Table I.

From Fig. 2, we observe that below the resonances, magic-wavelength B fields grow smaller with increasing laser frequency. This is a reflection of the fact that at small ω_L , the HFI-mediated polarizability approaches a constant value, while the vector polarizability $\propto \omega_L$. Thus, $B_m \propto 1/\omega_L$ in accord with Fig. 2. As the frequency is increased, the $B_m(\omega_L)$ increases near the atomic resonance (fine-structure doublet).

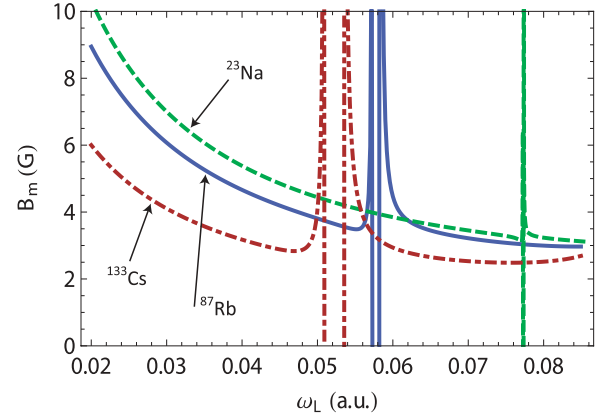


FIG. 2. (Color online) Dependence of magic B field (in G) on laser frequency (in atomic units) for ^{23}Na (dashed green line), ^{87}Rb (solid blue line), and ^{133}Cs (dot-dashed red line). Magic B fields for other isotopes of the same element may be obtained using the scaling law, Eq. (9).

This leads to a prominent elbow-like minimum in the $B_m(\omega_L)$ curves.

The magic B field has been recently measured for optical lattice-confined ^{87}Rb at 811.5 nm, Ref. [9]. At this wavelength and degree of circular polarization $A = 0.77(4)$, the measured $B_m = 4.314(3)\text{G}$. For a purely circularly polarized light, this translates into $B_m = 3.32(17)\text{G}$. The computed magic B field, 3.62G, is 1.8σ larger than the measured value.

A quick glance through the Table I reveals that the required B fields for ^{39}K are much weaker than for other alkali metals; this is related to the fact that the nuclear moment of this isotope is almost an order of magnitude smaller than that of other species. An additional suppression is due to the magic B fields being *quadratic* in hyperfine splitting (clock frequency).

Notice that if the B field and the direction of laser propagation are set at an angle θ , then $A \rightarrow A \cos \theta$ in Eq. (8) (see Ref. [7]). This angle provides an additional experimental handle on reaching the magic-wavelength conditions. Increasing the angle and reducing the degree of circular polarization raise the values of the magic B field.

Generically, the ratio $\alpha_{FF}^{(0),\text{HFI}}(\omega_L)/\alpha_{nS_{1/2}}^a(\omega_L)$ is on the order of a ratio of the hyperfine splitting to the fine-structure

TABLE I. Values of magic B fields for representative laser wavelengths. The optical field is assumed to be purely circularly polarized. Values of the clock transition frequencies ν_0 and the second-order Zeeman frequency shift coefficients $\delta\nu_Z/B^2$ are listed in the second and the third columns, respectively. Magic B fields for other isotopes of the same element may be obtained with the scaling law, Eq. (9).

	ν_0 (GHz)	$\delta\nu_Z/B^2$ (kHz/G ²)	Magic B (G)		
			10.6 μm	1.065 μm	811.5 nm
^7Li	0.80	4.9	—	144	64.9
^{23}Na	1.77	2.2	47.4	5.07	4.05
^{39}K	0.46	8.5	0.782	0.0848	0.0672
^{87}Rb	6.83	0.57	41.0	4.39	3.62
^{133}Cs	9.19	0.43	27.3	3.00	3.81

splitting in the nearest P -state manifold, i.e., it is much smaller than unity. This reinforces the validity of the weak-field approximation used to derive Eqs. (5) and (8). Notice, however, that $\lim_{\omega_L \rightarrow 0} \alpha_n^a S_{1/2}(\omega_L) \rightarrow 0$; this may lead to unreasonably large magic B fields for very low-frequency fields. Such a breakdown occurs for ${}^7\text{Li}$ at $10.6 \mu\text{m}$ in Table I.

It is worth pointing out that the results of Fig. 2 and Table I may be extended to other, e.g., unstable, isotopes. An analysis of the third-order expressions for the HFI-mediated polarizabilities shows that the magic B fields scale with the nuclear spin and g factor as

$$B_m \propto g_I^2 \frac{2I(2I+1)^2}{(2I+2)^{3/2}}. \quad (9)$$

Finally, I would like to comment on the magic conditions for the $M_F \neq 0$ states discussed in our earlier work [7]. The idea there was to rotate the bias B field with respect to the laser propagation. At a certain laser-frequency-dependent magic “angle”, $\theta \approx 90^\circ$, contributions of the HFI-mediated scalar polarizability and the rotationally suppressed vector polarizability were compensating each other. Notice that we may attain the Zeeman insensitivity even in this case. Indeed, in a magnetic field, two hyperfine levels $|F = I + 1/2, M_F\rangle$

and $|F = I - 1/2, M_F\rangle$ repel each other through off-diagonal Zeeman coupling. In addition, the g factors of the two levels have opposite signs. This leads to a minimum in the clock-frequency dependence on B fields. These minima occur at relatively large magnetic fields, e.g., about 2 kG for ${}^{87}\text{Rb}$. This $dv(B)/dB = 0$ condition fixes magic B field values for the proposal [7].

It is anticipated that a variety of applications could take advantage of the magic conditions computed in this paper. For example, the dynamic Stark shift is the primary factor limiting lifetime of quantum memory [5]; here an advance may be made by switching to the magic B fields. It remains to be seen if the micromagic lattice clock can be developed; here one needs to investigate the feasibility of stabilizing bias magnetic fields at the magic values. In this regard, notice that we still have a choice of fixing laser wavelength, polarization, and rotation angle to optimize clock accuracy with respect to drifts in the B field.

Acknowledgments. I thank Trey Porto, Nathan Lundblad, and Alex Kuzmich for discussions. This work was supported in part by the US NSF and by the US NASA under Grant/Cooperative Agreement No. NNX07AT65A issued by the Nevada NASA EPSCoR program.

-
- [1] J. Ye, H. J. Kimble, and H. Katori, *Science* **320**, 1734 (2008).
 [2] H. Katori, M. Takamoto, V. G. Pal’chikov, and V. D. Ovsiannikov, *Phys. Rev. Lett.* **91**, 173005 (2003).
 [3] A. D. Ludlow *et al.*, *Science* **319**, 1805 (2008).
 [4] K. Beloy, A. Derevianko, V. A. Dzuba, and V. V. Flambaum, *Phys. Rev. Lett.* **102**, 120801 (2009).
 [5] R. Zhao, Y. O. Dudin, S. D. Jenkins, C. J. Campbell, D. N. Matsukevich, T. A. B. Kennedy, and A. Kuzmich, *Nature Phys.* **5**, 100 (2009).
 [6] P. Rosenbusch, S. Ghezali, V. A. Dzuba, V. V. Flambaum, K. Beloy, and A. Derevianko, *Phys. Rev. A* **79**, 013404 (2009).
 [7] V. V. Flambaum, V. A. Dzuba, and A. Derevianko, *Phys. Rev. Lett.* **101**, 220801 (2008).
 [8] J. M. Choi and D. Cho, *J. Phys. Conf. Ser.* **80**, 012037 (2007).
 [9] N. Lundblad, M. Schlosser, and J. V. Porto, *Phys. Rev. A* **81**, 031611(R) (2010).
 [10] N. L. Manakov, V. D. Ovsiannikov, and L. P. Rapoport, *Phys. Rep.* **141**, 320 (1986).
 [11] X. Zhou, X. Chen, and J. Chen, e-print [arXiv:physics/0512244](https://arxiv.org/abs/physics/0512244).
 [12] K. Beloy, U. I. Safronova, and A. Derevianko, *Phys. Rev. Lett.* **97**, 040801 (2006).
 [13] S. G. Porsev, K. Beloy, and A. Derevianko, *Phys. Rev. Lett.* **102**, 181601 (2009).